HHS Public Access

Author manuscript

J Neurochem. Author manuscript; available in PMC 2015 November 04.

Published in final edited form as:

J Neurochem. 2008 November ; 107(3): 722–733. doi:10.1111/j.1471-4159.2008.05643.x.

Effects of γ-secretase cleavage-region mutations on APP processing and Aβ formation: interpretation with sequential cleavage and α-helical model

Jianxin Tan[*], **Guozhang Mao**[*], **Mei-Zhen Cui**[*], **Shin-Chung Kang**[†], **Bruce Lamb**[‡], **Boon-Seng Wong**[†,§], **Man-Sun Sy**[†], and **Xuemin Xu**[*]

[*]Department of Pathobiology, College of Veterinary Medicine, The University of Tennessee, Knoxville, Tennessee

[†]Department of Pathology, Case Western Reserve University, Cleveland, Ohio

[‡]Department of Neuroscience, Lerner Research Institute, Cleveland Clinic Foundation Cleveland, Ohio

[§]Department of Physiology, National University of Singapore, Singapore

Abstract

Overwhelming evidence supports the amyloid hypothesis of Alzheimer's disease that stipulates that the relative level of the 42 amino acid β-amyloid peptide ($A\beta_{42}$) in relationship to $A\beta_{40}$ is critical to the pathogenesis of the disease. While it is clear that the multi-subunit gamma secretase is responsible for cleavage of the amyloid precursor protein (APP) into $A\beta_{42}$ and $A\beta_{40}$, the exact molecular mechanisms regulating the production of the various Aβ species remain elusive. To elucidate the underlying mechanisms, we replaced individual amino acid residues from positions 43 to 52 of Aβ with phenylalanine to examine the effects on the production of $A\beta_{40}$ and $A\beta_{42}$. All mutants, except for V50F, resulted in a decrease in total Aβ with a more prominent reduction in Aβ for residues 45, 48, and 51, following an every three residue repetition pattern. In addition, the mutations with the strongest reductions in total Aβ had the largest increases in the ratio of $A\beta_{42}$/$A\beta_{40}$. Curiously, the T43F, V44F, and T48F mutations caused a striking decrease in the accumulation of membrane bound $A\beta_{46}$, albeit by a different mechanism. Our data suggest that initial cleavage of APP at the ε site is crucial in the generation of Aβ. The implicated sequential cleavage and an α-helical model may lead to a better understanding of the γ-secretase-mediated APP processing and may also provide useful information for therapy and drug design aimed at altering Aβ production.

Keywords

Alzheimer's disease; amyloid; amyloid precursor protein processing

Address correspondence and reprint requests to Xuemin Xu, PhD, 2407 River Dr, A201 Veterinary Teaching Hospital, Knoxville, TN 37996, USA. xmx@utk.edu.

Abnormal generation and accumulation of the β-amyloid peptide (Aβ) is thought to be the causative event in Alzheimer's disease (AD) pathogenesis (Hardy and Selkoe 2002). This amyloid hypothesis is specifically supported by the observations that all the mutations identified in the three AD genes [amyloid precursor protein (APP), presenilin-1 (PS1), and (PS2)] were found to cause abnormal Aβ formation, either by increasing total Aβ or increasing the ratio of $Aβ_{42}/Aβ_{40}$. Aβ is proteolytically derived from APP, which can be processed in two different pathways: the amyloidogenic pathway and the non-amyloidogenic pathway. In the amyloidogenic pathway, APP is first processed by β-secretase to produce a large, soluble ectodomain sAPPβ and a membrane-anchored C-terminal fragment (CTFβ). This CTFβ is subsequently processed by γ-secretase, resulting in the Aβ peptide and an APP intracellular domain (which is also known as CTFε as it is generated by the ε-cleavage of γ-secretase). In the non-amyloidogenic pathway, APP is first processed by α-secretase within the Aβ sequence to produce sAPPα and a membrane-associated CTFα, which undergoes further γ-secretase processing to result in the formation of p3 and CTFε. As γ-secretase cleavages generate the C-termini of Aβ and determine the ratio of $Aβ_{42}/Aβ_{40}$, the mechanism by which γ-secretase mediates processing of APP has been one of the focuses of AD research. Studying genetic, biological, and environmental factors that affect the γ-secretase-mediated cleavages of APP would provide important information on the development of treatment and prevention of the disease. In an effort to understand the molecular events of γ-secretase-mediated processing of APP, we recently identified a new ζ-cleavage site at $Aβ_{46}$ between the known γ-cleavage site at $Aβ_{40/42}$ and the ε-cleavage site at $Aβ_{49}$ (Zhao *et al.* 2004). More importantly, our finding that these cleavages can be differentially inhibited by different γ-secretase inhibitors made it possible to elucidate a sequential relationship of the cleavage cascade, i.e. ε-cleavage occurs first, followed by ζ-cleavage and γ-cleavage commencing at the site closest to the membrane boundary and proceeding toward the site in the middle of the transmembrane domain of APP (Zhao *et al.* 2005). These findings prompted us to determine how mutations around these cleavage sites, specifically those at upstream cleavage sites, affect the formation of Aβ. It should be pointed out that, before the discovery of the new ζ-cleavage site at $Aβ_{46}$, in most previous studies, the effects of genetic factors and pharmaceutical treatment on the specificity or preference of γ-secretase were determined by the formation of the final product, secreted $Aβ_{40/42}$, without considering the formation of the intermediate product $Aβ_{46}$. In this regard, it is especially important to determine the effects of APP mutations, which have been shown to alter the generation of secreted Aβ produced by γ-cleavage, on the upstream ε- and ζ-cleavages. In addition, precisely determining the levels of $Aβ_{40}$, $Aβ_{42}$ and other Aβ species produced from these interesting APP mutants is a key factor in determining the effects of APP mutations on the formation of Aβ. For this purpose, in the current study, we employed APP knockout cells to eliminate the interference of endogenous Aβ. To this end, we examined the effects of systematically engineered phenylalanine (F) mutations within the intramembrane region of multiple γ-secretase sites, which have been reported to have a pronounced effect on the generation of secreted Aβ without affecting the α-helical structure of the APP transmembrane domain (Lichtenthaler *et al.* 1999), on the upstream ε- and ζ-cleavages, and the formation of the intermediate long $Aβ_{46}$. We found that mutations that slow down ε-cleavage, the initial cleavage of the ε-, ζ-, and γ-cleavages, result in a decrease in Aβ formation. Our data also demonstrated that F-mutations caused a

progressive, stepwise reduction in total Aβ formation, and this reduction in total Aβ was observed every three residues within a region from $Aβ_{45}$ to $Aβ_{50}$. Furthermore, the F-mutations that caused a striking decrease in $Aβ_{40}/Aβ_{total}$ also caused a remarkable increase in the ratio of $Aβ_{42}/Aβ_{40}$ and $Aβ_{42}/Aβ_{total}$.

Materials and methods

General reagents

γ-Secretase inhibitors, N-[N-(3,5-difluorophenacetyl)-L-alanyl]-(S)-phenylglycine methyl ester (DAPM), compound E, and L-685, 458 were from Calbiochem (San Diego, CA, USA) and were dissolved in dimethylsulfoxide (Me_2SO). $Aβ_{40}$ and $Aβ_{42}$ were purchased from American Peptide (Sunnyvale, CA, USA). $Aβ_{46}$ is a customized peptide. Monoclonal antibody 6E10, which recognizes residues 1–17 of the Aβ sequence, and polyclonal antibody anti-Aph-1α, which is specific to the C-terminal of Aph-1αL, were from COVANCE (Dedham, MA, USA). Polyclonal antibody anti-nicastrin (NCT) was developed against a peptide corresponding to the C-terminal of NCT, which was purchased from Sigma (St Louis, MO, USA). APP N-terminal-specific antibody 22C11 was from Boehringer (Mannheim, Indianapolis, IN, USA). Polyclonal antibody C15 raised against the C-terminal 15 residues of human APP has been described previously (Zhao *et al.* 2004). Horseradish peroxidase conjugated anti-rabbit and anti-mouse antibodies, Protein-A agarose beads, and ECL-Plus western blotting reagents were all purchased from Amersham Biosciences (Piscataway, NJ, USA).

Plasmid construction and mutagenesis

The plasmid APPsw, which expresses a C-terminal truncated Swedish mutant APP (APPsw) (Thinakaran *et al.* 1996), was kindly provided by Dr Gopal Thinakaran (University of Chicago). All other site-directed mutations were made using APPsw as a template and using the Site-Directed mutaGenesis Kit (Stratagene, La Jolla, CA, USA).

Establishment of APP-knockout cell line

To establish $APP^{-/-}$−1 neuronal cell lines, the cerebellum was aseptically dissected from a 1-day-old $APP^{-/-}$−1 mouse and placed in cold phosphate-buffered saline containing sodium pyruvate, penicillin, and streptomycin. The tissues were minced and washed before being dissociated with trypsin–EDTA. After stopping the reaction with Dulbecco's modified Eagle's medium (DMEM), the tissues were sheared, centrifuged at 300 *g*, and resuspended in DMEM. Cell viability was determined using trypan blue before seeding at 1×10^5 cells/mL in growth medium (DMEM supplemented with HEPES, glucose, L-glutamine, sodium pyruvate, 10% fetal calf serum, penicillin, streptomycin, amphotericin B, insulin, selenium, and transferrin) in tissue culture flasks pre-coated with poly-L-lysine solution. Cells were cultured for 3 days in an incubator at 37°C with 5% CO_2. Cytosine arabinoside (10 μM) was then added to the culture for an additional 24 h to eliminate the dividing cells. Cells were then washed with medium and replenished with fresh medium. Visible colonies began to appear within 10–14 days after selection with cytosine arabinoside. We then immortalized this cell line by co-transfecting a plasmid (pSV40) that encodes the large T antigen alongside a second plasmid (pcDNA3.1) that encodes the hygromycin selection gene

using FUGENE 6 reagent (Roche, Indianapolis, IN, USA). The transfected clones were gradually selected with increasing amounts of hygromycin. We established one long-term culture line, $APP^{-/-}$−1. This cell line expresses high levels of microtubule associated protein-2 (MAP-2) but lacks nestin and β-3 tubulin. The microtubule associated protein-2 (MAP-2c, 70 kDa) isoform is expressed only in the newborn brain, and its level of expression is reduced by at least 10-fold in a 10- to 20-day-old brain. These results suggest that $APP^{-/-}$−1 is likely to be derived from an early neuronal progenitor (Kang, Lamb, Wong and Sy, unpublished results).

Cell culture, transfection, and treatment

Wild type mouse neuroblastoma N2a and the APP-knockout cell lines ($APP^{-/-}$−1) were grown in DMEM supplemented with 10% fetal bovine serum, 1% penicillin/streptomycin, and 1% L-glutamine. Using the liposome-mediated method, $APP^{-/-}$−1 cells were transfected using Lipofectamine 2000 (Invitrogen, Carlsbad, CA, USA) according to the manufacturer's instructions. Six hours after transfection, the medium was replaced, and the cells were cultured for an additional 30 h in the absence or presence of γ-secretase inhibitor as indicated for each specific experiment. Then, the media were collected for analysis of the secreted Aβ and soluble N-terminal fragment of APP (sAPP). The cells were harvested for analyses of the membrane-bound Aβ, full-length APP, APP CTFs, and γ-secretase components.

ELISA, immunoprecipitation, and western blot analysis

ELISA was performed using an $Aβ_{40}$-specific and $Aβ_{42}$-specific ELISA kit from Invitrogen following the instructions provided by the manufacturer. Immunoprecipitation and western blot analysis were carried out as described previously (Zhao *et al.* 2004). Briefly, secreted Aβ was immunoprecipitated from conditioned medium (CM) using a monoclonal Aβ-specific antibody 6E10 (COVANCE). The immunoprecipitates were analyzed by 11% Bicine/urea sodium dodecyl sulfate–polyacrylamide gel electrophoresis (SDS–PAGE) followed by western blotting. For detecting the membrane bound $Aβ_{46}$ and other APP derivatives, cells were lysed in western blotting lysis buffer (50 mM Tris–HCl, pH 6.8, 8 M urea, 5% β-mercaptoethanol, 2% SDS, and protease inhibitors) and separated by a 10%–16% two-step Tris–glycine SDS–PAGE system. After the samples were transferred to a polyvinylidene fluoride membrane (Immobilon-P; Millipore, Bedford, MA, USA), the membranes were probed with specific antibodies, and the immunoreactive bands were visualized using ECL-Plus (Amersham Biosciences).

Cell-free assay

The *in vitro* generation of CTFε (also known as APP intracellular domain) by γ-secretase was assayed in a cell-free assay system established previously (Pinnix *et al.* 2001), following the procedure described by Sastre *et al.* (2001) with minor modifications. Briefly, to determine the effect of APPsw and its F-mutations on the generation of CTFε, $APP^{-/-}$−1 cells were transiently transfected with APPsw and its F-mutations. After culturing 24 h, γ-secretase inhibitor DAPM was added, and cells were cultured for an additional 12 h. The cells were harvested in nine volumes of homogenization buffer [10 mM 4-

Morpholinepropanesulfonic acid (MOPS), pH 7.0, and 10 mM KCl] containing protease inhibitors (Complete; Roche, Indianapolis, IN, USA) and homogenized by passing through a 20-gauge needle 30 times. After the removal of unbroken cells and nuclei by centrifugation at 800 *g* at 4°C for 10 min, membranes were pelleted by centrifugation at 20 000 *g* at 4°C for 30 min. The membranes were washed once with homogenization buffer and resuspended in assay buffer (150 mM sodium citrate, pH 6.4, protease inhibitor cocktail). Aliquots of membranes were then incubated at 37°C for 2 h. Reactions were stopped by addition of SDS-loading buffer. After boiling for 5 min, the samples were analyzed with a 10–16% two-step Tris–glycine SDS–PAGE system followed by western blotting using C15, an antibody specific for the APP C-terminus.

Results

Characterization of APP knockout cell line

To eliminate the interference of the endogenous mouse App in our assays, we established the $APP^{-/-}$−1 cell line that does not express APP (see Materials and methods). The absence of endogenous APP in this cell line was first demonstrated by RT-PCR (not shown) and then confirmed by immunoblotting. The neuroblastoma N2a cells from the wild type $APP^{+/+}$ (APPwt) mouse was used as a control. As shown in the top panel of Fig. 1, when cell lysates from control cells were examined by western blot analysis using an APP C-terminal-specific antibody C15, two isoforms of endogenous APP (mainly 125 kDa and a trace amount of 110 kDa) were detected (lane 2). These proteins were not detected in the mock-transfected $APP^{-/-}$−1 cells (lane 3). Lane 4 is the lysate from $APP^{-/-}$−1 cells transfected with APPsw, which is a human APP with 695 amino acids containing the Swedish mutation, and is expressed with a myc tag fused to its C-terminal. As the two endogenous APP isoforms detected in the wild type N2a cells (lane 2) run more slowly than the human APP of 695 amino acids (lane 4), the two endogenous APP isoforms are apparently the APP751 of 751 amino acids and APP695 of 695 amino acids, respectively. As shown in the top panel, the APP CTF (mostly CTFα) was detected in wild type N2a cells (lane 2), but not in the $APP^{-/-}$−1 cells (lane 3). As expected, when the cells were cultured in the presence of γ-secretase inhibitors, such as L-685,458 or compound E, the CTFs were accumulated to a high level (lanes 5, 7, 8, and 10). Because the CTFs produced from human APPsw contain a myc tag, they have a slower migration rate than endogenous CTFs (compare lane 7 with lane 8, top panel). It was noted that in the absence of inhibitor, a modest level of endogenous CTFα was detected (top panel, lane 2), but almost no CTFs was detected in $APP^{-/-}$−1 cells transfected with APPsw (lane 4). One possible reason is that as APPsw is mostly processed by β-secretase and CTFβ is apparently a better substrate of γ-secretase, in the absence of inhibitor, almost all of the CTFβ was processed into Aβ, resulting in the undetectable CTFs.

On the other hand, when the CM from these cells were analyzed by western blotting using the APP N-terminal-specific antibody 22C11, which recognizes a region between amino acids 66 and 81 of APP (Weidemann *et al.* 1989; Hilbich *et al.* 1993), sAPP was detected in both wild type N2a cells (middle panel, lanes 2, 5, and 8) and the $APP^{-/-}$−1 cells transfected with APPsw (lanes 4, 7, and 10), but not in the mock-transfected $APP^{-/-}$−1 cells (lanes 3, 6, and 9). When the CM was immunoprecipitated by 6E10, which is an antibody specific for

residues 1–17 of human Aβ (Kim *et al.* 1990), secreted $Aβ_{38}$, $Aβ_{40}$, and a small amount of $Aβ_{42}$ were detected in cells transfected with APPsw (bottom panel, lane 4), indicating that this $APP^{-/-}$−1 cell line can process APP and produce Aβ. However, when the cells were cultured in the presence of γ-secretase inhibitors (bottom panel, lanes 7 and 10), secreted Aβ was almost completely abolished. Because of the extremely low affinity of 6E10 for the murine Aβ-containing peptide (Wang *et al.* 1996), no secreted Aβ was detected in wild type mouse cells, regardless of the presence (bottom panel, lanes 5 and 8) or absence (bottom panel, lane 2) of γ-secretase inhibitors.

As shown in Fig. 1b, when wild type N2a cells were transfected with APPsw, similarly, a high level of secreted Aβ was observed in APPsw-expressing cells (lane 2). However, when N2a cells were transfected with APPsw containing a phenylalanine substitution for threonine at position 48 of the Aβ sequence, APPsw (T48F), a dramatic decrease in $Aβ_{40}$ and a slight increase in $Aβ_{42}$ were observed (compare lane 3 with lane 2, bottom panel). As a result, a high level of accumulation of CTFβ/α was observed in T48F mutant-expressing cells in comparison with that in cells expressing APPsw (compare lane 3 with lane 2, top panel). As shown in Fig. 1c, when the $APP^{-/-}$−1 cells were transfected with APPwt, a much lower level of secreted Aβ was detected in comparison with that produced by APPsw-transfectant (compare lane 2 with lane 3). In addition, when the T48F mutation was introduced into APPwt, the resulting APP(T48F) mutant produced even less secreted Aβ (lane 1). Taken together, these data clearly demonstrate that the $APP^{-/-}$−1 cell does not express endogenous APP, but is able to normally process exogenously expressed APP by α-, β-, and γ-secretases and produce Aβ and other APP metabolites as the wild type cells do. Therefore, to amplify the readout signal (the secreted Aβ) and to eliminate the interference of the endogenous APP, we used $APP^{-/-}$−1 cells and APPsw expression constructs to study the effects of mutations within the region of γ-secretase-mediated cleavage sites on Aβ formation and the sequential ε-, ζ-, and γ-cleavage cascade.

Phenylalanine substitutions for residues flanking the ζ- and ε-cleavage site have strong effects on the turnover of the APP CTFs (α and β) and on the formation of secreted Aβ

We recently reported that the C-termini of Aβ are generated by a series of sequential γ-secretase-mediated cleavages, i.e. ε-cleavage at $Aβ_{49}$ followed by ζ-cleavage at $Aβ_{46}$ and then by γ-cleavage at $Aβ_{40/42}$ (Zhao *et al.* 2005). This finding prompted us to determine whether and how the mutations around the two upstream cleavage sites, namely the ζ-cleavage site and the initial ε-cleavage site, influence the sequential ε-, ζ-, and γ-cleavages and the formation of Aβ. For this purpose, a series of site-directed point mutations was created in APPsw by individually substituting F for the residues at positions $Aβ_{43}$–$Aβ_{52}$. $APP^{-/-}$−1 cells were transiently transfected with each of the F-mutants. Immunoblotting of cell lysates of these transfectants with antibody C15 showed that equal levels of the mutant proteins were expressed in $APP^{-/-}$−1 cells [panel (a) of Fig. 2]. It was noted that some of these mutants [V44F, I45F, V46F, T48F, and L49F (Fig. 2a lanes 4, 5, 6, 8, and 9)] caused an accumulation of CTFα and CTFβ (mostly CTFα). As shown in panels Fig. 2(b, c, and d), no significant difference was observed in the levels of sAPP (sAPPα and sAPPβ) nor in the γ-secretase components, such as NCT, Aph-1α (APH1), Pen-2 (PEN2), and PS-1 (PS1N) among the F-mutants. These results clearly indicate that these F-mutations have no effects

on α- and β-cleavage. PS was detected using an antibody specific for the N-terminal of PS-1 (Xu *et al.* 2002). Actin was used as an internal loading control (panel Fig. 2e).

Next, the secreted Aβ produced by these transfected cells was determined by immunoprecipitation and western blot analysis. As shown in Fig. 3a, all F-mutants are processed by γ-secretase to generate secreted Aβ species, albeit with different efficiencies. It was noted that F-mutation V46F at the P1 position of the ζ-cleavage site [P positions on the substrate are counted from the point of cleavage; P1 is the first residue towards the N-terminal, and the P1′ position is the first residue towards the C-terminal side of a cleavage site. For P nomenclature, see (Schechter and Berger 1967)] and F-mutation L49F at the P1 position of the ε-cleavage site caused a significant decrease in $A\beta_{40}$ and a concomitant increase in $A\beta_{42}$ in comparison with cells expressing native APPsw (compare lanes 6 and 9 with lane 2). F-mutations at the P2 position of these cleavage sites, I45F and T48F, caused a further decrease in $A\beta_{40}$ and a concomitant increase in $A\beta_{42}$ (lanes 5 and 8). When the residues at the P1′ position of these cleavage sites, $A\beta_{47}$ and $A\beta_{50}$, were replaced with phenylalanine, the F-mutations I47F and V50F caused a dramatic decrease in $A\beta_{42}$ (lanes 7 and 10). Interestingly, in the V44F mutant-expressing cells, instead of $A\beta_{40}$ and $A\beta_{42}$, significant amounts of $A\beta_{38}$ and $A\beta_{41}$ were detected (lane 4). A small amount of $A\beta_{41}$ was also detected in cells expressing I47F mutant. $A\beta_{38}$ was detected in all cell lines. However, in cells, which express F-mutants that caused an increase in $A\beta_{42}$ (or $A\beta_{41}$), a higher level of $A\beta_{38}$, sometimes both $A\beta_{38}$ and $A\beta_{39}$, was detected. There are also a band likely $A\beta_{37}$ detected in most of the cells, but a high level of $A\beta_{37}$ was detected in the F-mutant cells that produced higher level of $A\beta_{40}$ (such as V50F, lane 10). These observations suggest a product–precursor relationship between $A\beta_{38(39)}$ and $A\beta_{42(41)}$ and between $A\beta_{37}$ and $A\beta_{40}$.

We next carried out a quantitative analysis of the effects of these F-mutations on the generation of the secreted major Aβ species $A\beta_{40}$ and $A\beta_{42}$ using commercially available ELISA specific for $A\beta_{40}$ and $A\beta_{42}$ (Invitrogen). As shown in Fig. 3b, these F-mutations had different effects on the ratio of $A\beta_{42}/A\beta_{40}$. The highest ratio of $A\beta_{42}/A\beta_{40}$ was observed in cells transfected with I45F mutant. As this ELISA kit specifically detects only $A\beta_{40}$ and $A\beta_{42}$, the quantitative analysis of total Aβ and also the next abundant species $A\beta_{38}$ were quantified by densitometric analysis of the western blot results shown in Fig. 3a. The results are summarized in Fig. 3c. First, as shown in panel (iv) of Fig. 3c, except for mutant V44F, the effects of these F-mutants on the ratio of $A\beta_{42}/A\beta_{40}$ was observed as a pattern exactly the same as the one shown in Fig. 3b, indicating that the densitometric analysis is equally as accurate as ELISA. As shown in Fig. 3a, in some of the mutant-expressing cells (specifically mutants V44F and I47F), instead $A\beta_{42}$, $A\beta_{41}$ was detected, we defined the *y*-axis as $A\beta_{42(41)}/A\beta_{40}$; this accounts for the only difference between Fig. 3b and panel (iv) of Fig. 3c. As shown in Fig. 3c, most of the F-mutations, except V50F, caused a decrease in the total Aβ [Fig. 3c, panel (i)]. Among them, the mutations that caused a strong decrease in $A\beta_{40}$ also caused a strong decrease in total Aβ. Furthermore the F-mutations from V50F to T48F caused a progressive stepwise reduction in total Aβ formation. A similar progressive reduction in total Aβ formation was also observed from I47F to I45F and from L52F to M51F. Interestingly, a similar interval repetition (every three residues) of the progressive reduction in the ratio of $A\beta_{40}/A\beta_{total}$ was also observed from L52F to I45F [Fig. 3c, panel

(ii)]. In contrast, as shown in panel Fig. 3c(iii), an opposite interval repetition of the progressive decrease in the ratio of $A\beta_{42(41)}/A\beta_{total}$ was observed from I45F to L52F [Fig. 3c, panel (iii)]. A similar progressive decrease in the ratio of $A\beta_{42(41)}/A\beta_{40}$ [Fig. 3c, panel (iv)] and $A\beta_{38}/A\beta_{total}$ [Fig. 3c, panel (v)] was observed as well. On the other hand, the effects of T43F and V44F mutations did not follow the interval repeating pattern [Fig. 3c, panels (i–v)]. Interestingly, it was noted that substitution of phenylalanine at position $A\beta_{44}$ resulted in the formation of $A\beta_{41}$ instead of $A\beta_{42}$ (Fig. 3a, lane 4). $A\beta_{40}$ was also dramatically decreased, and $A\beta_{38}$ became the major species of the secreted Aβ. Moreover, it was noted that $A\beta_{41}$ is different from $A\beta_{40}$, which is mainly secreted before being further processed. However, $A\beta_{41}$ is more like $A\beta_{42}$ and is further processed into $A\beta_{38}$ rather than being secreted. Therefore, we grouped $A\beta_{41}$ with $A\beta_{42}$ rather than $A\beta_{40}$ in Fig. 3c. The T43F mutation caused a slight increase in $A\beta_{42}$, but a decrease in $A\beta_{40}$ (Fig. 3a, lane 3).

T48F, T43F, and V44F mutations caused a significant decrease in the formation of $A\beta_{46}$

As reported previously, $A\beta_{40}$ and $A\beta_{42}$ are produced from CTFβ mediated by the formation of their intermediate precursor $A\beta_{46}$ (Zhao *et al.* 2005, 2007); next, we examined the effects of these F-mutants on the formation of $A\beta_{46}$. To do so, mutants expressing $APP^{-}/^{-}$−1 cells were treated with γ-secretase inhibitor compound E, which inhibits the turnover of $A\beta_{46}$ and causes an accumulation of CTFα/β (Zhao *et al.* 2004). As shown in panel (a) of Fig. 4, in the presence of compound E, accumulation of CTFα/β was observed in all APP variants (lanes 2–12). As shown in the bottom of panel (b) of Fig. 4, when cells were cultured in the presence of compound E, a significant amount of membrane-bound $A\beta_{46}$ was detected in cells expressing APPsw (lane 2) and in most of the F-mutant-expressing cells, except the cells expressing T43F (lane 3), V44F (lane 4), and T48F (lane 8) mutants, in which $A\beta_{46}$ level was very low. In addition, a significant decrease in $A\beta_{46}$ was observed in cells expressing I47F (lane 7) and M51F (lane 11) mutants, and a modest decrease in $A\beta_{46}$ was observed in cells expressing I45F (lane 5), V46F (lane 6), and L49F (lane 9) mutants. The $A\beta_{46}$ level remained unchanged in V50F and L52F mutant-expressing cells (lanes 10 and 12).

T48F mutation significantly reduced efficiency of ε-cleavage

We next performed a cell-free assay to determine how these F-mutants affect the upstream ε-cleavage. $APP^{-/-}$−1 cells transfected with a control APPsw or F-mutants were cultured in the presence of the γ-secretase inhibitor DAPM for 12 h [DAPM has been used for accumulating CTFα/β in previous studies (Zhao *et al.* 2005, 2007)]. Membranes were prepared, and the cell-free assays were carried out as described in the Materials and methods. As shown in Fig. 5, when these membranes were incubated at 37°C for 2 h, a significant amount of CTFε was detected in the membranes prepared from all cells except cells expressing T48F mutant. In spite of the high level of CTFα/β accumulated, only a very low level of CTFε was detected in the membranes prepared from T48F mutant-expressing cells (lane 8), indicating that this T48F mutant is not efficiently processed by γ-secretase at the ε-cleavage site. This low efficient upstream ε-cleavage may, at least in part, account for the very low level of $A\beta_{46}$.

T43F and V44F mutants are less sensitive to γ-secretase inhibitor compound E

As shown in panel (b) of Fig. 4, almost no detectable $A\beta_{46}$ was observed in cells expressing T43F (lane 3) or V44F (lane 4) mutants in the presence of compound E, which is known to inhibit the turnover of $A\beta_{46}$. As these mutations did not cause a reduction of CTFε (Fig. 5), the low level of $A\beta_{46}$ must not be because of the inhibition of upstream ε- and ζ-cleavages, as seen in the case of the T48F mutant. One possibility is that, when these mutations are present, compound E may be unable to block the γ-cleavage at $A\beta_{40/42}$, and as a result, the intermediate $A\beta_{46}$ is further processed into $A\beta_{40/42}$. To test this possibility, $APP^{-/-}$−1 cells were transfected with APPsw, T43F, V44F, I45F, and V46F (APPsw, I45F, and V46F were used as controls) and then cultured in the presence or absence of compound E. The secreted Aβ was immunoprecipitated from the CM of each cell line. As shown in Fig. 6, in the absence of an inhibitor, secreted Aβ was detected in all transfectants (lanes 7–11). When the cells were cultured with compound E, almost no secreted Aβ was detected in cells expressing APPsw (lane 2), I45F (lane 5), and V46F (lane 6) mutants. However, a significant amount of each of the secreted Aβ species ($A\beta_{38}$, $A\beta_{40}$, $A\beta_{41}$, and $A\beta_{42}$) was detected in the media of cells expressing T43F (lane 3) and V44F (lane 4) mutants. These results indicate that the Aβ formation from these mutants is less sensitive to the inhibitory effects of compound E.

Discussion

Characterization of APP knockout cell line

A key factor in determining the effects of APP mutations on the formation of Aβ or in understanding the preference of γ-secretase cleavage is to precisely determine the levels of $A\beta_{40}$, $A\beta_{42}$, and other Aβ species produced from these interesting APP mutants. In most previous studies, these kinds of experiments were carried out in a model using cells that express endogenous APP. However, the most widely used methods, including ELISA and western blotting, are based on the use of specific antibodies that cannot distinguish the Aβ produced from exogenous mutant APP from that of endogenous APPwt. To eliminate the interference of endogenous APP, we established an APP knockout ($APP^{-/-}$) cell line, $APP^{-/-}$−1. As shown in Fig. 1, in $APP^{-/-}$−1 cells neither full-length APP nor its derivatives were detected by APP-specific antibodies. The results presented in Fig. 1 also demonstrate that when the $APP^{-/-}$−1 cells were transfected with APPsw, the exogenous APP was processed normally by all the α-, β-, and γ-secretases. Specifically, it was clearly demonstrated that secreted Aβ species were produced from the exogenous APPsw and that the production of secreted Aβ and the turnover of CTFα and CTFβ were inhibited by γ-secretase inhibitors. Hence, the $APP^{-/-}$−1 cell line is a useful tool for studying the mechanism of γ-secretase-mediated Aβ formation. Using this model, we examined the effects of mutations within the region of the γ-secretase cleavage sites on the processing of APP and the generation of Aβ.

Phenylalanine-mutations within the region of multiple γ-secretase sites have different effects on the formation of different Aβ species, but follow an ordered pattern

We and others recently identified long forms of Aβ species $A\beta_{46}$ (Zhao *et al.* 2004; Qi-Takahara *et al.* 2005). The identification of the long Aβ species led to the discovery of a new

ζ-cleavage site at $A\beta_{46}$ between the known γ-cleavage site at $A\beta_{40/42}$ and ε-cleavage site at $A\beta_{49}$ (Zhao *et al.* 2004). Specifically, the finding that some of the known γ-secretase inhibitors can block the formation of short forms of $A\beta_{40/42}$ and cause a concomitant accumulation of the long form of $A\beta_{46}$, suggests a possible precursor–product relationship between $A\beta_{46}$ and $A\beta_{40/42}$ (Zhao *et al.* 2004). Indeed, the precursor–product relationship between $A\beta_{46}$ and $A\beta_{40/42}$ has been experimentally determined using the differential inhibition strategy (Zhao *et al.* 2005) and further confirmed by the pulse-chase labeling experiment (Zhao *et al.* 2007). These observations established a sequential cleavage model, i.e. the C-terminus of secreted Aβ is generated by γ-secretase via a series of sequential cleavages, first by ε-cleavage at $A\beta_{49}$, followed by ζ-cleavage at $A\beta_{46}$ and then γ-cleavage at $A\beta_{40/42}$ (Fig. 7) (Zhao *et al.* 2005, 2007). These events commence at the site closest to the membrane boundary and proceed toward the site in the middle of the membrane domain of APP (Zhao *et al.* 2005). Thus, the altered generation of secreted Aβ caused by some factors may be a result of influencing upstream cleavages. However, before the discovery of the new ζ-cleavage site at $A\beta_{46}$, in most previous studies, the effects of genetic mutations on the formation of Aβ were determined by the detection of the final product, $A\beta_{40/42}$, without considering the formation of the intermediate product, $A\beta_{46}$. In this regard, it is especially important to determine the effects of APP mutations within the intramembrane region of multiple γ-secretase sites on the upstream ε- and ζ-cleavages and the formation of the intermediate long $A\beta_{46}$. For this purpose, we systematically substituted individual F residues within the intramembrane region of multiple γ-secretase sites. The reason for choosing F-mutation is based on the previous observation that F-mutations have a pronounced effect on the generation of secreted Aβwithout affecting the α-helical structure of the APP transmembrane domain (Lichtenthaler *et al.* 1999).

What have we learned from these experiments? First, the pattern of the effects of these F-mutations on the ratio of $A\beta_{42}/A\beta_{40}$ observed in this study is very similar to that observed in a previous study (Lichtenthaler *et al.* 1999). In addition, we observed that almost no $A\beta_{40}$ was detected in I45F mutant-expressing cells and that instead of $A\beta_{42}$, $A\beta_{41}$ was detected in V44F mutant-expressing cells, similar to previous observations (Lichtenthaler *et al.* 1999). However, there are also some significant differences between the current and previous studies. First, our data clearly demonstrated that most of the F-mutations caused a decrease in the levels of total Aβ and some of them, such as I45F and T48F, reduced total Aβ up to 50% (Fig. 3a and c). These observations are different from a previous study, in which no significant differences in the level of total Aβ were observed in these F-mutants (Lichtenthaler *et al.* 1999). One possibility is that COS7 (African Green Monkey SV40-transf'd kidney fibroblast cell line) cells were used in the previous study, and the endogenous Aβ, which is identical to human Aβ, may have interfered with the detection and quantification of Aβ produced from cells transfected with F-mutant APP. Secondarily, in the previous study, it was reported that a very low amount of Aβ was detected in cells transfected with the L52F mutant (Lichtenthaler *et al.* 1999), and this has been imputed to the possible rapid degradation of the precursor protein A4CT-L52F, in which the large aromatic phenylalanine at the membrane boundary position might interfere with the correct membrane insertion of A4CT-L52F (Lichtenthaler *et al.* 1999). However, our data clearly demonstrated that the L52F mutation caused only slight reduction in total Aβ (< 10%, Fig.

3c). These differences might have resulted from different constructs being used in these two studies. In the previous study, the plasmid SPA4CT, which expresses CTFβ with a signal peptide, was used to create the F-mutations and transfect COS7 (African Green Monkey SV40-transf'd kidney fibroblast cell line) cells (Lichtenthaler *et al.* 1999). In our study, the plasmid APPsw, which expresses full-length APPsw, was used to create the F-mutations and transfect $APP^{-/-}$−1 cells. However, whether this particular L52F mutation has a different effect on the membrane insertion of these two polypeptides expressed by these two different constructs is currently not clear. Thirdly, in the previous study, a significant amount of $Aβ_{40}$ was detected in V44F mutant cells (Lichtenthaler *et al.* 1999). However, in the current study, only a trace amount of $Aβ_{40}$ was detected in V44F mutant cells (Fig. 3a). This difference may have resulted from the gel system used. The gel system used in the previous study could not separate $Aβ_{40}$ from $Aβ_{38}$, and this may account for the overestimation of $Aβ_{40}$.

Observations from our current study and the previous study revealed some interesting findings: First, a novel finding revealed by our results was that the F-mutations at different positions caused a decrease in total Aβ to a different extent, and the effects of these F-mutations on the decrease in total Aβ followed a well-ordered pattern; i.e. a progressive, stepwise reduction in total Aβ formation was observed every three residues within a region from $Aβ_{45}$ to $Aβ_{50}$, and it could possibly extend to $Aβ_{52}$; Second, the effects of these F-mutations on the ratio of $Aβ_{40}/Aβ_{total}$ precisely followed the same every three residues interval pattern as the total Aβ. Third, these F-mutations had opposite effects on the ratio of $Aβ_{42}/Aβ_{40}$, $Aβ_{42}/Aβ_{total}$, and $Aβ_{38}/Aβ_{total}$; i.e. the mutations, which caused a strong decrease in total Aβ and the ratio of $Aβ_{40}/Aβ_{total}$, resulted in a strong increase in the ratio of $Aβ_{42}/Aβ_{40}$, $Aβ_{42}/Aβ_{total}$, and $Aβ_{38}/Aβ_{total}$. Fourth, T43F, V44F, and T48F mutations caused a striking decrease in the accumulation of membrane bound $Aβ_{46}$ using different mechanisms as discussed below.

Mechanisms underlying the effects of F-mutations on the formation of Aβ

To understand the mechanism by which APP is processed by γ-secretase within its transmembrane domain, an α-helical model of the APP transmembrane domain was proposed in previous studies (Lichtenthaler *et al.* 1999; Wolfe *et al.* 1999). Based on recent findings, we adapted the α-helical model to recently suggest that the same γ-secretase is responsible for the multiple intramembrane cleavages of APP (Zhao *et al.* 2005, 2007). The proposed α-helical structure of the APP transmembrane domain and the single enzyme model may also provide an explanation for the every three residue repetition effect of these F-mutations on Aβ formation observed in this study. First, how do some of the F-mutations cause a strong increase in the ratio of $Aβ_{42}/Aβ_{40}$? As shown in Fig. 8a, in their native state, the peptide bonds, which are hydrolyzed by γ-secretase to produce the major intermediates $Aβ_{46}$ and $Aβ_{43}$, are aligned on the same side of the α-helical wheel, which may be the enzyme targeting side. This may explain the fact that the $Aβ_{46}$ generated by ζ-cleavage is mostly cleaved at $Aβ_{43}$ to produce $Aβ_{43}$ that is further mainly processed at $Aβ_{40}$ to produce $Aβ_{40}$, which is the major secreted Aβ species under normal physiological conditions. However, $Aβ_{46}$ may also be cleaved with lower efficiency at $Aβ_{42}$. Specifically, under some circumstances, such as unknown environmental factors and mutations in both APP and PS,

which may cause conformational changes, altering the relative position of the enzyme attacking site, the efficiency of cleavage at $A\beta_{42}$ may be increased. For example, as shown in Fig. 8b, if this relative positional change between APP and the γ-secretase complex can be mimicked by rotating the α-helical wheel clockwise to a certain degree, the peptide bond between residues $A\beta_{43}$ and $A\beta_{42}$ would move toward the center of the enzyme attacking site and become more susceptible to the γ-secretase cleavage, resulting in an increase in $A\beta_{42}$. When the F-mutations cause the preference shift in favor of cleavage at $A\beta_{42}$, the cleavage at $A\beta_{43}$ would be reduced, resulting in a decrease in $A\beta_{40}$, which is formed from $A\beta_{43}$. This model provides a mechanism by which F-mutations cause a striking increase in the ratio of $A\beta_{42}/A\beta_{total}$ resulting in a drastic concomitant decrease in the ratio of $A\beta_{40}/A\beta_{total}$. In this regard, it was noted that F-mutations I45F, T48F, and M51F, which caused stronger increases in $A\beta_{42}/A\beta_{total}$, are aligned on the same side of the α-helical wheel, providing a possible explanation for the interval (every three residues) repetition pattern of the effects of these F-mutations on Aβ formation. As the F-mutations that caused a shift in the preference of the γ-secretase cleavage may have altered the native relative position of the substrate to the enzyme, the efficiency of the γ-secretase cleavage may have been reduced. This reduced cleavage efficiency may account for the fact that F-mutations that caused a striking increase in the ratio of $A\beta_{42}/A\beta_{40}$ also caused a marked reduction in total Aβ.

It was noted that the striking increase in the ratio of $A\beta_{42}/A\beta_{40}$ is mostly due to the marked reduction in $A\beta_{40}$ rather than an increase in the level of $A\beta_{42}$. One possibility for the fact that striking decrease in $A\beta_{40}$ is not accompanied with significant increase in $A\beta_{42}$ is that as $A\beta_{42}$ is longer than $A\beta_{40}$, which is mostly released with limited further processing into $A\beta_{37}$ (see Fig. 2a, lanes 10 and 12, for example), most of the $A\beta_{42}$ is not released from the γ-secretase complex immediately after being formed, but is further processed mostly into $A\beta_{38}$ (possibly also into $A\beta_{39}$, see Fig. 2a, lanes 5 and 11) as proposed in a previous study (Zhao *et al.* 2007). This conclusion is also supported by our finding that the modest increase in $A\beta_{42}$ was always accompanied by an increase in $A\beta_{38}$ or $A\beta_{39}$. This may also be explained by the α-helical wheel model, in which the peptide bond between residues $A\beta_{43}$ and $A\beta_{42}$ and the peptide bond between residues $A\beta_{39}$ and $A\beta_{38}$ are aligned on the same side. If the mutations render the peptide bond between residues $A\beta_{43}$ and $A\beta_{42}$ more susceptible to γ-secretase cleavage, the peptide bond between residues $A\beta_{39}$ and $A\beta_{38}$ would also become more susceptible to γ-secretase cleavage. Accordingly, the V44F mutation may have caused a further relative conformational change between substrate and enzyme by rotating the α-helical wheel to a position at which the peptide bond between residues $A\beta_{42}$ and $A\beta_{41}$ can be cleaved by γ-secretase; accordingly, the peptide bond between residues $A\beta_{39}$ and $A\beta_{38}$ would also become more susceptible to γ-secretase cleavage, leading to the formation of $A\beta_{41}$ and even more $A\beta_{38}$ (Fig. 2a, lane 4).

In contrast to the V44F, I45F, and T48F mutations, which caused a decrease in the ratio of $A\beta_{40}/A\beta_{total}$ and in the level of total Aβ, mutations I47F, V50F, and L52F, which had no significant effects in the level of total Aβ and the ratio of $A\beta_{40}/A\beta_{total}$ but caused a decrease in the ratio of $A\beta_{42}/A\beta_{total}$, may just have the opposite effect on the relative conformation between substrate and enzyme, by rotating the α-helical wheel counterclockwise. This

change would push the peptide bond between $A\beta_{42}$ and $A\beta_{43}$ further away from the center of the enzyme-attacking site, resulting in a decrease in $A\beta_{42}$ and its derivative $A\beta_{38}$ or $A\beta_{39}$.

The other possibility that may account for the effects of certain F-mutations on the cleavage preference shift from $A\beta_{40}$ to $A\beta_{42}$ is the model proposed by a recent study that indicates there are two product lines: one is a major line that starts with the formation of $A\beta_{49}$ with subsequent turnover of $A\beta_{49}$ into $A\beta_{46}$ to $A\beta_{43}$ to $A\beta_{40}$; the other line is started with the formation of $A\beta_{48}$ with subsequent turnover of $A\beta_{48}$ to $A\beta_{45}$ to $A\beta_{42}$ to $A\beta_{38}$ (Qi-Takahara *et al.* 2005). However, as shown in Fig. 8b, when the peptide bond between $A\beta_{42}$ and $A\beta_{43}$ is aligned to the center of the enzyme-attacking site, the peptide bond between $A\beta_{48}$ and $A\beta_{49}$ is still not in the favorable position. Furthermore, even in the case of an F-mutation, such as I45F mutation, that caused a striking increase in the $A\beta_{42}/A\beta_{40}$ ratio, the intermediate detected is $A\beta_{46}$ rather than $A\beta_{45}$ (Fig. 4), indicating that the formation of $A\beta_{45}$ is not necessary for the formation of $A\beta_{42}$. Therefore, even the two product lines model cannot be ruled out, it may not be the major mechanism that accounts for the increase in $A\beta_{42}$ caused by the F-mutations tested in this study.

As mentioned above, it was found that T43F, V44F, and T48F mutations caused a striking decrease in the accumulation of membrane bound $A\beta_{46}$ using different mechanisms. The observations that T48F mutation caused an increase in the accumulation of CTFα/β (Fig. 2a) as well as a dramatic decrease in CTFε production (Fig. 5), strongly suggest that this T48F mutation causes reduction in the bound intermediate $A\beta_{46}$ most likely by inhibiting the ε-cleavage, which is the initial and rate determining step of the γ-secretase-mediated sequential cleavage cascade (Zhao *et al.* 2005).

On the other hand, T43F and V44F mutations did not inhibit the generation of CTFε, indicating that these mutations have no effect on the upstream ε-cleavage. In contrast, the observation that secreted Aβ was detectable in cells expressing these mutations even in the presence of compound E (Fig. 6) strongly suggests that these mutants are no longer sensitive to compound E, which block the turnover of the intermediate $A\beta_{46}$ by inhibiting the downstream γ-cleavage at $A\beta_{40/42}$ (Zhao *et al.* 2005). One possible reason for this insensitivity is that the introduction of this large amino acid at these positions obstructed compound E from approaching the γ-cleavage site, either by causing a local conformational change between the substrate and enzyme or by functioning as a barrier; as a result, $A\beta_{46}$ was further processed into secreted Aβ species.

I47F and M51F mutations also caused a modest decrease in the accumulation of membrane-bound $A\beta_{46}$ (Fig. 4). The fact that no significant reduction of CTFε was observed in a cell-free assay (Fig. 5) suggests the modest reduction in $A\beta_{46}$ is not due to the inhibition of ε-cleavage as T48F mutation does. In addition, secreted Aβ was not detected in the presence of compound E (data not shown). These observations suggest that the mechanism causing the decrease in accumulation of membrane-bound $A\beta_{46}$ in I47F and M51F is different from the ones accounting for the effects of T43F, V44F, and T48F mutations. One possible reason is that these mutations, by themselves, may have no inhibitory effect on the ε-cleavage. However, in the presence of these mutations, the inhibitor compound E, which usually does

not inhibit the formation of $A\beta_{46}$, may exhibit an inhibitory effect on the ε-cleavage and, as a result, block the formation of $A\beta_{46}$.

It has been proposed previously that γ-secretase may contain a PS dimer as the core of the enzyme (Schroeter *et al*. 2003). Whether this PS dimer may provide more than one catalytic site and account for the multiple cleavages of APP transmembrane domain remain to be determined.

Acknowledgments

This work was supported by Grants from NIH (R01AG026640) and the Alzheimer's Association (IIRG-05-14584) to XX and Grants from NIH (R01HL074341) to M-ZC.

Abbreviations used

AD	Alzheimer's disease
AICD	APP intracellular domain
APP	amyloid precursor protein
APPsw	Swedish mutant APP
APPwt	wild type APP
Aβ	β-amyloid peptide
CM	conditioned media
CTF	C-terminal fragment
DMEM	Dulbecco's modified Eagle's medium
NCT	nicastrin
PS	presenilin
sAPP	soluble APP
SDS-PAGE	sodium dodecyl sulfate–polyacrylamide gel electrophoresis

References

Hardy J, Selkoe DJ. The amyloid hypothesis of Alzheimer's disease: progress and problems on the road to therapeutics. Science. 2002; 297:353–356. [PubMed: 12130773]

Hilbich C, Monning U, Grund C, Masters CL, Beyreuther K. Amyloid-like properties of peptides flanking the epitope of amyloid precursor protein-specific monoclonal antibody 22C11. J Biol Chem. 1993; 268:26571–26577. [PubMed: 7504673]

Kim KS, Wen GY, Bancher C, Chen CMJ, Sapienza VJ, Hong H, Wisniewski HM. Detection and quantitation of amyloid B-peptide with 2 monoclonal antibodies. Neurosci Res Commun. 1990; 7:113–122.

Lichtenthaler SF, Wang R, Grimm H, Uljon SN, Masters CL, Beyreuther K. Mechanism of the cleavage specificity of Alzheimer's disease gamma-secretase identified by phenylalanine-scanning mutagenesis of the transmembrane domain of the amyloid precursor protein. Proc Natl Acad Sci USA. 1999; 96:3053–3058. [PubMed: 10077635]

Pinnix I, Musunuru U, Tun H, Sridharan A, Golde T, Eckman C, Ziani-Cherif C, Onstead L, Sambamurti K. A novel gamma-secretase assay based on detection of the putative C-terminal

fragment-gamma of amyloid beta protein precursor. J Biol Chem. 2001; 276:481–487. [PubMed: 11035007]

Qi-Takahara Y, Morishima-Kawashima M, Tanimura Y, et al. Longer forms of amyloid beta protein: implications for the mechanism of intramembrane cleavage by gamma-secretase. J Neurosci. 2005; 25:436–445. [PubMed: 15647487]

Sastre M, Steiner H, Fuchs K, Capell A, Multhaup G, Condron MM, Teplow DB, Haass C. Presenilin-dependent gamma-secretase processing of beta-amyloid precursor protein at a site corresponding to the S3 cleavage of Notch. EMBO Rep. 2001; 2:835–841. [PubMed: 11520861]

Schechter I, Berger A. On the size of the active site in proteases. I Papain. Biochem Biophys Res Commun. 1967; 27:157–162. [PubMed: 6035483]

Schroeter EH, Ilagan MX, Brunkan AL, et al. A presenilin dimer at the core of the gamma-secretase enzyme: insights from parallel analysis of Notch 1 and APP proteolysis. Proc Natl Acad Sci USA. 2003; 100:13075–13080. [PubMed: 14566063]

Thinakaran G, Teplow DB, Siman R, Greenberg B, Sisodia SS. Metabolism of the “Swedish” amyloid precursor protein variant in neuro2a (N2a) cells. Evidence that cleavage at the “beta-secretase” site occurs in the Golgi apparatus. J Biol Chem. 1996; 271:9390–9397. [PubMed: 8621605]

Wang R, Sweeney D, Gandy SE, Sisodia SS. The profile of soluble amyloid beta protein in cultured cell media. Detection and quantification of amyloid beta protein and variants by immunoprecipitation-mass spectrometry. J Biol Chem. 1996; 271:31894–31902. [PubMed: 8943233]

Weidemann A, Konig G, Bunke D, Fischer P, Salbaum JM, Masters CL, Beyreuther K. Identification, biogenesis, and localization of precursors of Alzheimer’s disease A4 amyloid protein. Cell. 1989; 57:115–126. [PubMed: 2649245]

Wolfe MS, Xia W, Moore CL, Leatherwood DD, Ostaszewski B, Rahmati T, Donkor IO, Selkoe DJ. Peptidomimetic probes and molecular modeling suggest that Alzheimer’s gamma-secretase is an intramembrane-cleaving aspartyl protease. Biochemistry (Mosc). 1999; 38:4720–4727.

Xu X, Shi YC, Gao W, Mao G, Zhao G, Agrawal S, Chisolm GM, Sui D, Cui MZ. The novel presenilin-1-associated protein is a proapoptotic mitochondrial protein. J Biol Chem. 2002; 277:48913–48922. [PubMed: 12377771]

Zhao G, Mao G, Tan J, Dong Y, Cui MZ, Kim SH, Xu X. Identification of a new presenilin-dependent ζ-cleavage site within the transmembrane domain of amyloid precursor protein. J Biol Chem. 2004; 279:50647–50650. [PubMed: 15485850]

Zhao G, Cui MZ, Mao G, Dong Y, Tan J, Sun L, Xu X. γ-Cleavage is dependent on ζ-cleavage during the proteolytic processing of amyloid precursor protein within its transmembrane domain. J Biol Chem. 2005; 280:37689–37697. [PubMed: 16157587]

Zhao G, Tan J, Mao G, Cui MZ, Xu X. The same gamma-secretase accounts for the multiple intramembrane cleavages of APP. J Neurochem. 2007; 100:1234–1246. [PubMed: 17241131]

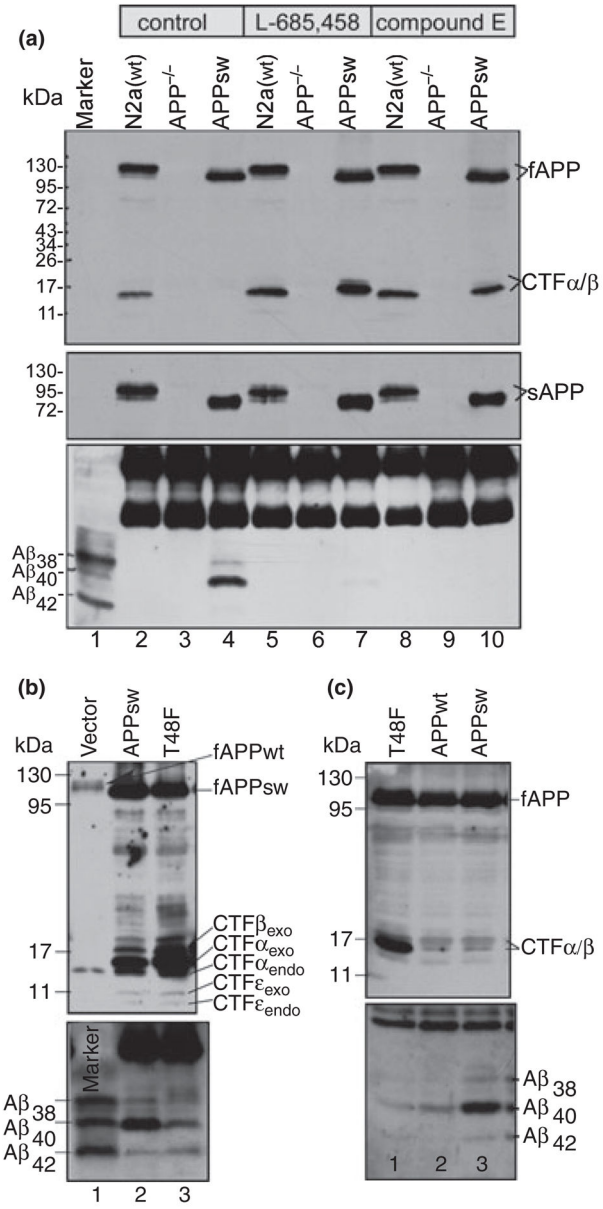

Fig. 1.

Characterization of the APP$^{-/-}$−1 cell line. (a) the APP$^{-/-}$−1 cells transiently transfected with APPsw and the wild type neuroblastoma N2a cells were cultured in the presence or absence of γ-secretase inhibitor, L685, 458 or compound E (indicated on top of the figure). Total lysates and conditioned media were analyzed by 10–16% (for lysates, top panel) and 10% (for media, middle panel) SDS–PAGE and probed with antibody C15 (for lysate) and 22C11 (for media), respectively. Both endogenous and exogenous full-length APP and CTFs (top panel), and soluble APPα/β (middle panel) were detected by C15 and 22C11, respectively. The secreted Aβs immunoprecipitated from the conditioned media were separated by 11% Bicine/urea SDS–PAGE and probed with 6E10 (bottom panel). Note: a large amount of Aβ was detected only in the conditioned media of the APPsw-transfected APP$^{-/-}$−1 cells cultured in the absence of any inhibitors (bottom panel, lane 4). Note: the

major endogenous APP isoforms is apparently the APP751 of 751 amino acids, which is larger than the recombinant APPsw that is created from APP695 of 695 amino acids. Thus, as shown in the top and middle panels, the endogenous fAPP and sAPP run slower than their counterparts of recombinant APPsw. (b) Wild type N2a cells were transfected with empty vector (lane 1), APPsw (lane 2), and APPsw containing T48F mutation (lane 3). (c) $APP^{-/-}$−1 cells were transfected with plasmid expressing Swedish mutant APPsw (lane 3), wild type APPwt (lane 2), and APPwt containing T48F mutation (lane 1).

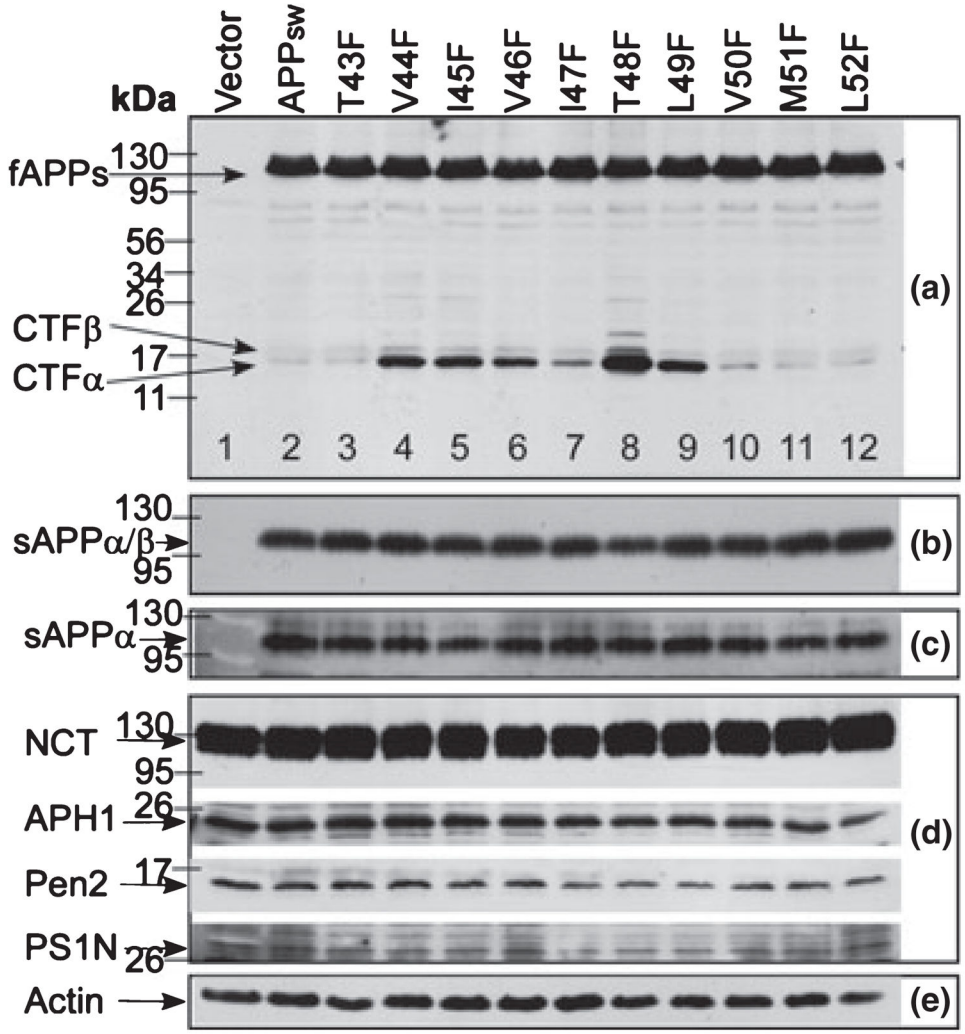

Fig. 2.

Effects of the substitutions of phenylalanine (F) for residues within a region of the γ-secretase multiple cleavage sites on the turnover of the APP C-terminal fragments (CTFα and CTFβ). The APP$^{-/-}$1 cells transiently transfected with APPsw and its F-mutants were cultured for 36 h. Cell lysates (panels a, d, and e) or the conditioned media (panels b and c) were separated by 10–16% or 10% SDS–PAGE, respectively, and probed with the following specific antibodies: C15 (panel a), 22C11(panel b), 6E10 (panel c), antibodies against components of γ-secretase complex (panel d: anti-NCT, anti-APH1α, anti-Pen2, and anti-PS1N), and anti-actin (panel e). 22C11 detects both sAPPα and sAPPβ (panel b); 6E10 detects sAPPα only (panel c). Lane 1 in all panels are samples from the mock-transfected APP$^{-/-}$1 cells.

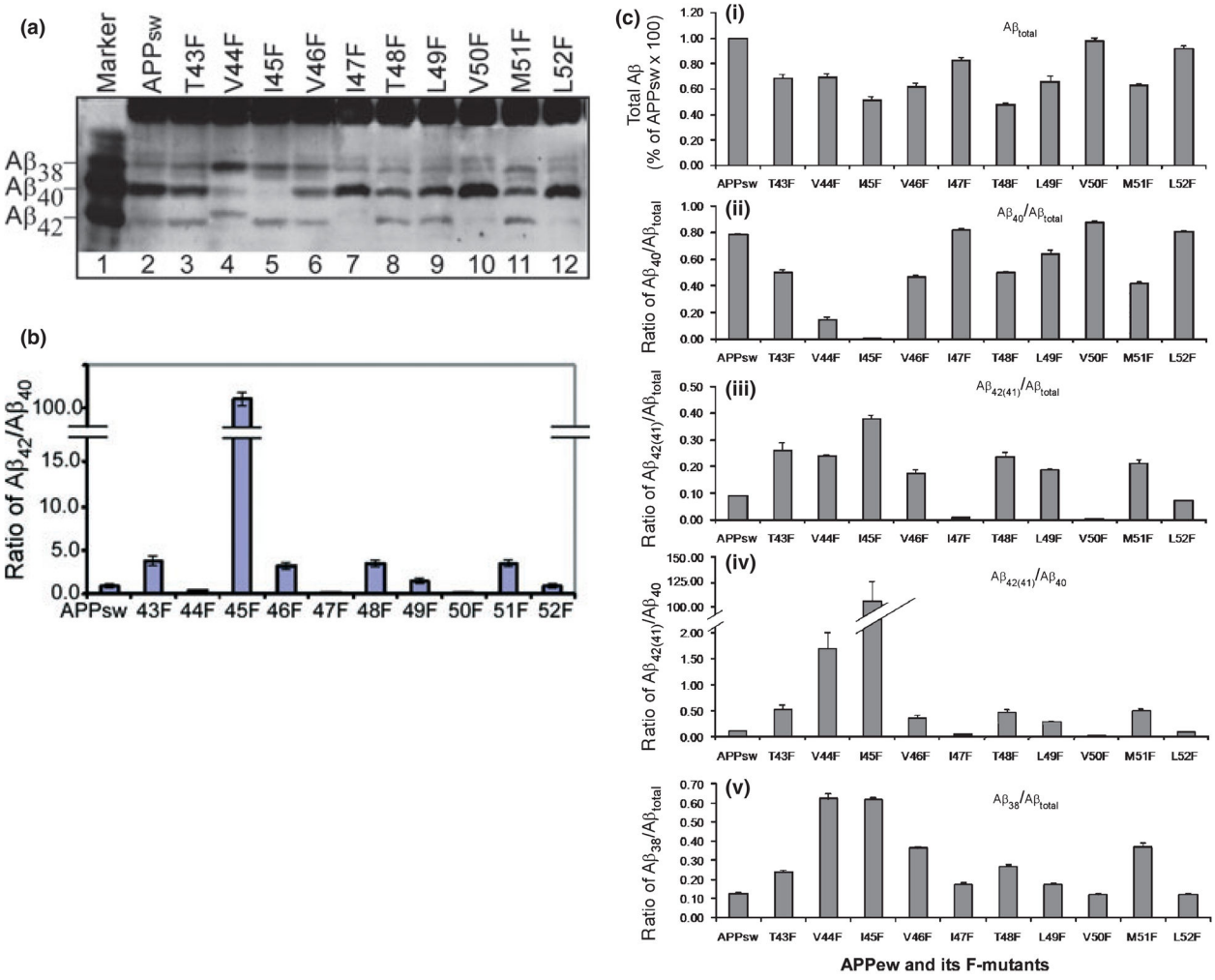

Fig. 3.

Effects of the substitutions of phenylalanine (F) for residues within a region of the γ-secretase multiple cleavage sites on the formation of secreted Aβ. (a) The APP$^{-/-}$1 cells transiently transfected with APPsw and its F-mutants were cultured for 36 h. The secreted Aβs immunoprecipitated from conditioned media were separated on 11% Bicine/urea SDS–PAGE and probed with 6E10. Lane 1 is the mixture of standard $Aβ_{38}$, $Aβ_{40}$, and $Aβ_{42}$ markers. (b) Ratio of $Aβ_{42}/Aβ_{40}$ determined by ELISA (representative of three repeated experiments). (c) Graphs represent the average of the results of densitometic analysis of three repeated western blots shown in (a). The density of each band was measured, and the ratios were calculated using the Gel Digitizing Software UN-SCAN-IT (Silk Scientific, Orem, UT, USA). Data from the ratio of total Aβ (panel i); $Aβ_{40}/Aβ_{total}$ (panel ii); $Aβ_{42(41)}/Aβ_{total}$ (panel iii); $Aβ_{42(41)}/Aβ_{40}$ (panel iv); and $Aβ_{38}/Aβ_{total}$ (panel v) are expressed as the mean ± SEM, n = 3. Note that the V44F mutant produced $Aβ_{41}$ instead of $Aβ_{42}$. The amount of Aβ generated was normalized to the expression level of each particular APP variant.

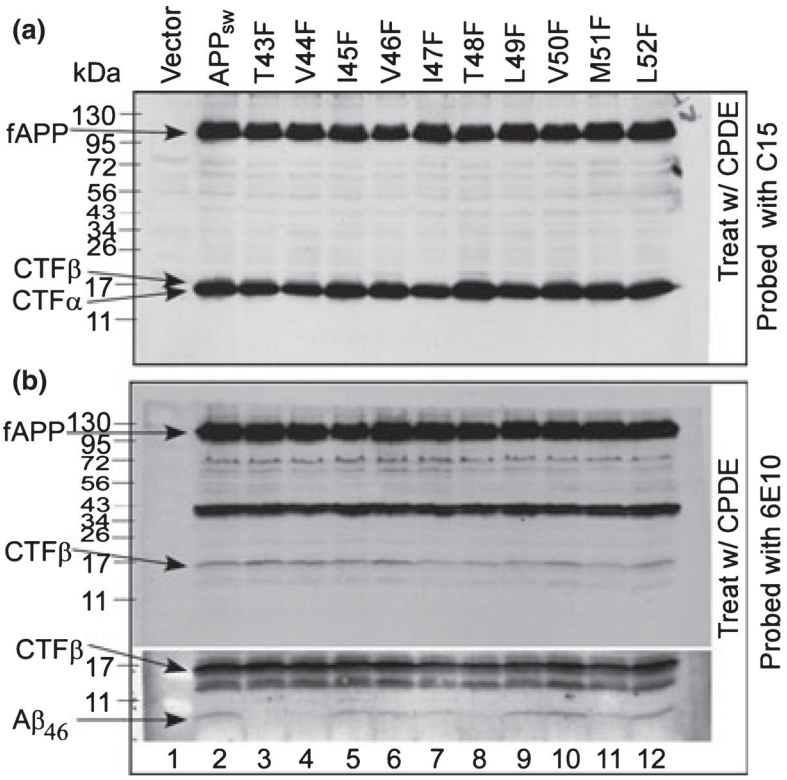

Fig. 4.

The effects of γ-secretase inhibitor compound E on the formation of $A\beta_{46}$ from APPsw and its F-mutants. The $APP^{-/-}$−1 cells transiently transfected with APPsw and its F-mutants were treated with γ-secretase inhibitor compound E for 12 h. Cell lysates were analyzed by 10–16% SDS–PAGE and probed with C15 (panel a) or 6E10 (panel b). Lane 1 includes the lysates of $APP^{-/-}$−1 cells transfected with pcDNA3.1 vector only. Lanes 2–12 are the lysates of $APP^{-/-}$−1 cells transfected with APPsw and its F-mutants as labeled on top of the figure. The bottom section in panel (b) is the longer exposure of the lower half of the upper section to visualize the membrane-bound $A\beta_{46}$.

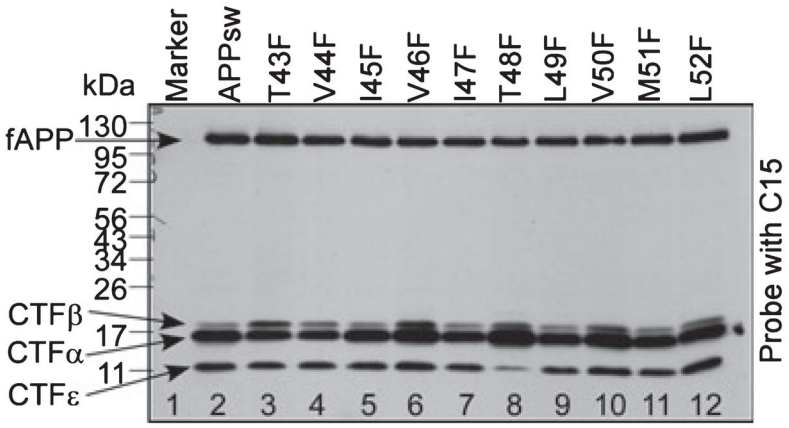

Fig. 5.

T48F mutation inhibits ε-cleavage. A cell-free assay was performed as described in the Materials and methods. Reaction mixtures were separated by 10–16% SDS–PAGE followed by western blot analysis.

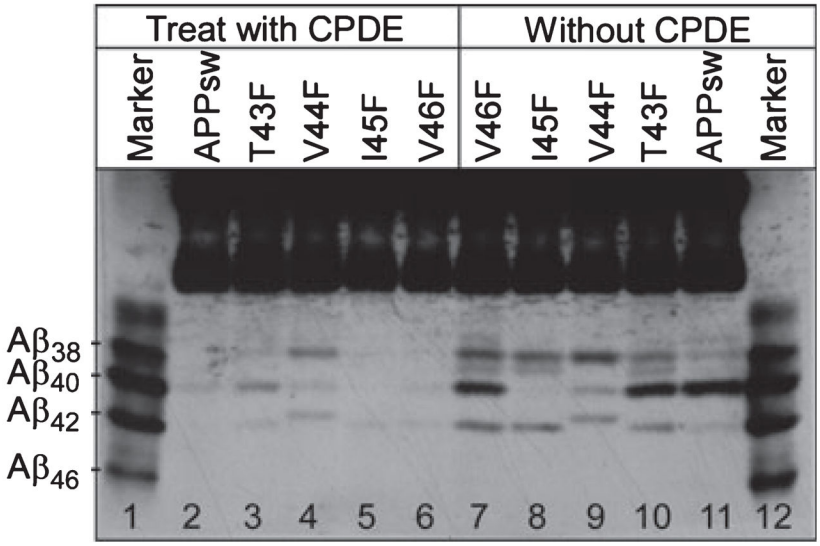

Fig. 6.

The T43F and V44F mutants are less sensitive to γ-secretase inhibitor compound E. APP$^{-}/^{-}$−1 cells transfected with APPsw, T43F, V44F, I45F, or V46F were cultured in the presence (lanes 2–6) or absence (lanes 7–11) of compound E for 24 h. The secreted Aβs were immunoprecipitated with 6E10 from the conditioned media, analyzed by 11% Bicine/urea SDS–PAGE, and probed with 6E10.

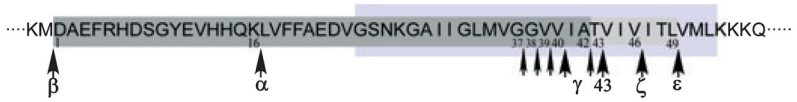

Fig. 7.

Schematic illustration of APP processing and Aβ formation. The C-termini of secreted Aβ are generated by γ-secretase via a series of sequential cleavages, first by ε-cleavage at $Aβ_{49}$, followed by ζ-cleavage at $Aβ_{46}$ to produce the major intermediate $Aβ_{46}$. $Aβ_{46}$ is mainly processed at $Aβ_{43}$ and the resulting $Aβ_{43}$ is further processed into $Aβ_{40}$, which can be further processed into $Aβ_{37}$, but is principally released from the γ-secretase complex and become the major form of secreted Aβ species. Alternatively, $Aβ_{46}$ can also be processed at $Aβ_{42}$ at a low efficiency and the resulting $Aβ_{42}$ can be either further processed into $Aβ_{38(39)}$ or released at a low rate. Amino acids are numbered based on Aβ sequence. The light gray represents the membrane; the dark gray shaded region is the Aβ sequence.

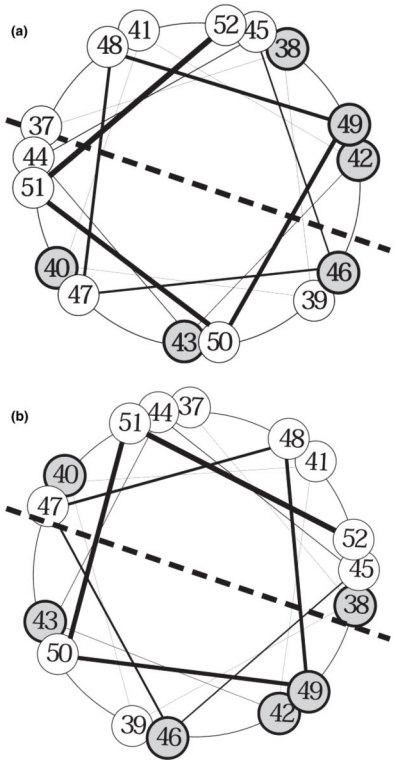

Fig. 8.

Helical wheel arrangement of amino acids 37–52 of CTFβ, a view from the cytosol side. The C-terminal residues of the major detectable Aβ species produced by γ-secretase-mediated cleavages are shown in gray with a bold outline. (a) Note that, under normal conditions, the peptide bond between residues 46 and 47 and the peptide bond between residues 43 and 44 are aligned to the center of the lower half of the α-helical wheel, which may be the enzyme attacking site. It is noted that the peptide bond between $A\beta_{39}$ and $A\beta_{40}$ is also aligned to the center of the lower half of the wheel. However, under normal conditions, the $A\beta_{40}$ resulting from cleavage at $A\beta_{40}$ is rapidly released from the γ-secretase complex, the peptide bond between $A\beta_{39}$ and $A\beta_{40}$ has less chance to be cleaved. In contrast, under some circumstances, such as environmental or genetic abnormalities, specifically, in the presence of mutations in presenilin or in APP, the relative position between the γ-secretase active site and its substrate may be altered during the assembly of the γ-secretase complex and its substrate. (b) If these changes in the position of CTFβ relative to the γ-secretase active site can be mimicked by rotating the CTFβ α-helical wheel clockwise 60°, the peptide bond between $A\beta_{42}$ and $A\beta_{43}$ will move toward the center of the lower half of the wheel and become much more susceptible to γ-secretase activity, resulting in an increase in the formation of $A\beta_{42}$.